AN EXPLORATION OF BINDER JETTING OF COPPER

Yun Bai and Christopher B. Williams

Design, Research, and Education for Additive Manufacturing Systems Laboratory

Department of Mechanical Engineering

Virginia Polytechnic Institute and State University

REVIEWED

Abstract

The ability to fabricate geometrically complex copper shapes via Additive Manufacturing (AM) could have a significant impact on the design and performance of thermal management systems and structural electronics. In this research a Binder Jetting AM process (ExOne R2) was used to fabricate green parts made of high purity copper powder. Once printed, the green part was sintered under a reducing atmosphere to create copper parts in pure metal form. The authors varied (i) powder size, (ii) sintering profiles, and (iii) atmospheric control to explore their effects on final part density and shrinkage. The sintered part density was 85% of the theoretical value due to the relatively coarse powder and loose packing of the powder bed. The result demonstrates the feasibility of using Binder Jetting to create copper parts with complex geometries.

1. Introduction

1.1 Motivation for the Additive Manufacturing of copper

One of the research opportunities identified in the 2009 Roadmap for Additive Manufacturing was to use Additive Manufacturing (AM) to create complex heat exchangers to enable a new generation of power generators for portable electronic devices that use hydrocarbon fuel cells [1]. Hydrocarbon fuels have higher energy density than batteries, but one challenge facing the use of hydrocarbon fuel in electronic devices lays in the thermal management where heat loss needs to be minimized. Copper, a highly conductive material, could be used to fabricate the reactor, which would feature complex intake and exhaust passages that can minimize heat losses via heat recirculation.

However, advances in the design of highly efficient thermal management systems are somewhat stymied by an inability to Additively Manufacture complex structures with copper material. To release this design constraint, the authors are investigating the use of Binder Jetting to process copper. This layer by layer fabrication process offers the utmost design freedom in the realization of complex geometries.

1.2 Current copper Additive Manufacturing technologies

Pure copper material has been fabricated with Additive Manufacturing processes including Laser Sintering (LS), Electron Beam Melting (EBM) and Ultrasonic Object Consolidation (UOC).

Laser Sintering (LS) has been used to indirectly fabricate metal parts from metal-polymer powders [2,3]. In their work, Badrinarayan and Barlow used LS to fabricate copper parts by selectively laser-scanning a bed of a copper-polymer (PMMA) powder mixture to melt the polymer layer-by-layer and create copper green parts. The copper green parts are then fired at elevated temperature to burn off the polymer, which acted as an intermediate binder, and sintered in a reducing atmosphere. This process was shown to create copper parts with density of 48% of the theoretical value, and up to 60% if using bimodal powders.

Copper components and open-cellular copper structures have been successfully created via Electron Beam Melting (EBM) from atomized copper precursor powders [4–6]. Copper oxide precipitates, and a novel columnar architecture by the reorganization of these precipitates, was observed due to the affinity of oxygen of finely atomized copper. In another study of processing pure copper parts via EBM, copper lattice structures and a near fully dense copper parts (99.8% of the theoretical density) were achieved via EBM [7,8]. The authors noted that the resultant parts suffered from dimensional inaccuracy (more than 13%) and contained pores and bubbles. These defects are believed to be caused by the severe dissipation of thermal energy during the melting process due to the high thermal conductivity of copper.

Ultrasonic Object Consolidation (UOC), a laminate-based AM process that features stacking, joining, and machining 2D laminates, has been used to fabricate copper parts. Tapes of copper were successively stacked and joined via ultrasonic welding, in which the recrystallized fine grains were converted from coarse-grained structures [9–11].

1.3 Rationale of Binder Jetting of copper

In this paper the authors explore the use of Binder Jetting to create copper parts. Binder Jetting is an Additive Manufacturing process in which a liquid binding agent is selectively deposited to join powder materials (Figure 1) [12]. In the green part creation stage, an inkjet printhead selectively deposits binder droplets into a powder bed and the binder interacts with the powder particles to form primitives that stitch together to form a cross-sectional layer. Once a layer has been printed, the powder feed piston raises, the build piston lowers, and a counter-rotating roller spreads a new layer of powder on top of the previous layer. The subsequent layer is then printed and is stitched to the previous layer by the jetted binder. The remaining loose powder in the bed supports overhanging structures and is removed with compressed air in post-processing. The green parts are then heated at an elevated temperature to cure the binder, which gives the parts sufficient strength for cleaning and handling. The printed parts require sintering to obtain the final density and strength. During sintering, the binder burns off and then particles sinter together through atomic diffusion.
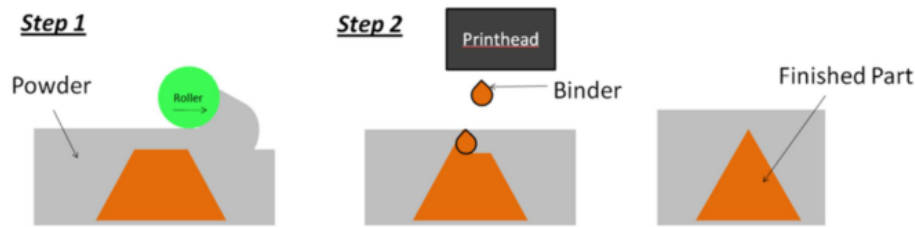
Figure 1. Binder jetting schematic [13]

Binder Jetting has several characteristics that make it well-suited for fabricating complex copper geometries:

- Its use of a powder bed eliminates the need for support structures typically required creating for overhanging features. While other direct-metal AM systems employ a powder bed, they require additional structures for part anchoring or heat dissipation purposes. Since Binder Jetting does not require such structures, this effectively eliminates the effort of printing and removing support structures.
- Binder Jetting is readily adaptable to a wide-range of materials [14]. Material development for direct-metal AM systems is typically hindered by concerns over a material's melt point, reactivity, optical reflectivity, and thermal conductivity. A variety of material systems, including polymer [15–19], ceramic materials [20], metals [21], and foundry sand [13,22] have been adapted to Binder Jetting.
- As it does not require an enclosed chamber, and does not use expensive energy sources, Binder Jetting is an inherently scalable technology. Binder Jetting systems have large build volumes; for example, ExOne offers build volumes of up to 780 x 400 x 400 mm for metal powders [36]; VoxelJet offers a "continuous" sand printer that does not restrict the length of its prints (at a 850 x 500 mm print width and height [37]). These large part sizes are possible as Binder Jetting is free from the powder bed thermal management constraints typically found in direct-metal AM processes. Furthermore, Binder Jetting systems have a relatively high throughput: a 100 nozzle printhead can create parts at up to ~200 cm^3/min.
- As Binder Jetting of metal functionally separates part creation from powder sintering, one can leverage understanding gained from well-studied traditional powder metallurgy (P/M) processes.

1.4 Context

In this paper, the authors present the results of their preliminary exploration of processing copper via Binder Jetting. Green parts were first fabricated by printing three different atomized copper powders (median size ranging from 15 to 75 μm) with an ExOne R2 3D printer. The green parts were then sintered in a tube furnace featuring a controlled atmosphere. The experimental procedure (Section 2) followed an established process for developing new materials for Binder Jetting, which included experiments in binder selection, powder formulation, powder-binder interaction testing and printing, and post-processing [14,23]. The resultant copper parts were characterized for sintered density, shrinkage, porosity, chemical composition, and ultimate tensile strength (Section 3). A summary of the work is presented in

Section 4 along with a discussion on future work on how to overcome the challenges encountered in Binder Jetting copper.

2. Experimental procedure

Given the authors' goal of processing copper via Binder Jetting, they followed Utela and coauthors' [23] established methodology for developing new materials for Binder Jetting. The methodology includes the selection of binder and powder, the determination of printing parameters in order to fabricate green parts, and the determination of the appropriate post-process sintering cycle. In this section, the specific experimental procedure for each stage of the development process is presented.

2.1 Binder selection

The criteria for binder selection for Binder Jetting focused on (i) binder interaction with candidate powders (wettability and penetration) and (ii) binder residue in the debinding post-process. The authors chose to work with ExOne's standard binder (PM-B-SR-1-04), as it is widely used binding agent for many metal powders and has been shown to have minimal ash residue during debinding.

The functional ingredient of the binder is a thermosetting polymer that can react to form polyester resins, which harden upon heating. The printed parts are cured at 190 °C for two hours to fully set the binder and provide satisfactory green part strength. The TGA analysis has demonstrated the binder can completely burn off at 450 °C.

2.2 Powder selection

Powders are selected based on their particle size distribution, morphology and chemical composition. In P/M, fine powder is preferred in order to lower the required sintering temperature and to improve densification. However, in Binder Jetting, particles larger than 20 μm are typically preferred so that the powder can be successfully spread during the recoating step [24]. Small particles can be used, however they need to be controlled in a small volume percentage and generally cannot be smaller than 1 μm [23,24,34]. A spherical particle shape is preferred over irregular shape because it tends to flow during recoating and it also is more easily wetted with binders.

Given these considerations, the authors chose gas atomized copper powder that features spherical particle shapes for Binder Jetting of copper. Three different powders were explored in order to determine the effect of powder size distribution on part processing: AcuPowder 153A copper powder, AcuPowder 500A ultra-fine atomized copper powder, and Ozometal atomized copper powder.

The particle size distribution of received powders was analyzed by laser scattering (Horiba LA-950 Laser Scattering Particle Size Distribution Analyzer). A FEI Quanta 600 FEG Environmental Scanning Electron Microscope (ESEM) using a voltage of 20 kV revealed the particle shape and verified particle size information by taking microscopic pictures of discrete

particles. The chemical composition was determined by Energy-dispersive X-ray spectroscopy (Bruker EDX) using the same voltage in ESEM.

The strength of the green part, and ultimately the quality of the final sintered part, is determined primarily by the green part density. This density is directly dependent on the density of the powder bed of the machine, which is affected both by powder characteristics and recoating parameters (e.g., the rotational and translational velocities of the counter-rotating spreading mechanism). To evaluate the powder bed packing density, the authors printed a density measuring cup into the powder bed, as shown in Figure 2. The mass of the packed powder that was in the cup was then measured. The packing density was then calculated as the ratio of the mass of the poured powder and the known volume of the density measuring cup. This method was also used to estimate the packing density for calculating the binder saturation (section 2.3).
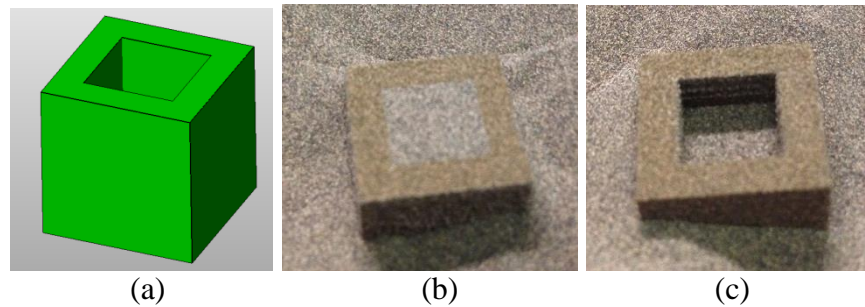

(a)   (b)   (c)

Figure 2. Powder bed packing density measurement method: (a) CAD file of the density measuring cup with a known volume. (b) The printed density measuring cup with packed powder. (c) The packed powder was emptied from the cup to measure the packing density

2.3 Green part creation

The compatibility of the received powder with the ExOne metal binder was tested by a bench top powder-liquid interaction test before the printing [23]. A pile of powder was strafed with a syringe of the binder liquid. The absorption rate of binder and the effectiveness of bounding particles were examined.

The critical printing parameters in the green body creation include layer thickness and binder saturation ratio. For a successful recoating of powders in Binder Jetting, the layer thickness should be at least thicker than the largest particle and preferably three times of particle size [25]. Saturation ratio (S) describes the percentage of the air space between powder particles (V_{air}) that is occupied by a binder volume (V_{binder}). The saturation ratio is determined from Equations (1) and (2), and is based on the packing density of the powder bed (*PR*) and the volume of solid particles in a defined envelope (V_{solid}). From these measurements, the ExOne R2 printing software calculates the required volume of binder to be printed once the binder saturation is input by the user.

$$S = V_{binder}/V_{air} \qquad (1)$$
$$V_{air} = (1 - \frac{PR}{100}) \times V_{solid} \qquad (2)$$

Saturation needs to be carefully selected as it affects the quality of printed green parts as well as the final sintered density. Sufficient binder saturation is required to obtain green part strength.

Conversely, oversaturation of the powder results in dimensional inaccuracy and low sintered density because of bonding unwanted loose powders and the resulting porosity following binder burn-out. For spherical particles, the binder saturation is relatively low because it uses binders efficiently by having small necking area between particles [26].

The layer thickness and the binder saturation of each copper powder were determined experimentally based on these criteria. The binder saturation was estimated first based on the observation from the powder-binder interaction test. The specimens with different combinations of layer thickness and binder saturation were printed iteratively until satisfactory green part quality and strength were observed.

2.4 Post-processing

To determine the suitable sintering profile for each powder, and to investigate how sintered densities are affected by sintering temperature, time and atmosphere, rectangular sintering test coupons ($24 \times 8 \times 4$ mm) were printed from each powder. The density and dimensions of each coupon were measured before and after the sintering to evaluate densification and shrinkage.

The solid state sintering of copper was conducted in a MTI GSL-1600X tube furnace (101 mm tube O.D.) in either air with a vacuum or in a controlled hydrogen/argon atmosphere as shown in Table 1.

Table 1. The atmospheres used for sintering copper

Atmosphere	Flow rate (ml/min) or vacuum (torr)
Hydrogen/Argon	100/0, 80/20, 60/40, and 20/80
Air	10-200 torr

When post-processing the parts in an air/vacuum environment, the heating schedule consisted of two primary stages: debinding and sintering. A 30 minute hold occurred at 450 °C to ensure removal of the printed binder. The temperature and time of the sintering stage (Figure 3a) was varied in order to explore its effect on sintered part density. Heating ramps of 5 °C /min and a cooling ramp of 5 °C /min were used to transition between stages. When post-processing in a reducing environment (Section 3.3), the heating stage featured three steps (Figure 3b). The additional step was held at 700 °C to facilitate the reduction of copper oxides before the closure of pores.
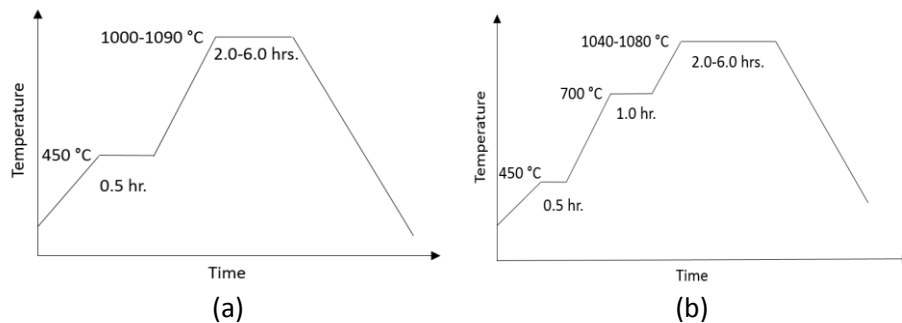

Figure 3. The heating schedule used for sintering copper (a) in air/vacuum and (b) in reducing atmosphere

2.5 Part characterization

The densification of copper was evaluated by comparing powder packing density, green density and final density. The green and sintered density was measured by a helium gas pycnometer (micromeritics AccuPyc II 1340) and a density measurement kit using Archimedes' principal (Denver Instrument). The sample mass was measured by an analytical balance (ACCULAB AL-64). Helium gas pycnometry measures the total displaced skeletal volume of the sample [27]. Archimedes' principle measures the volume of water displaced by an immersed object, of which the surface pores were sealed by oil impregnation before measurements [28]. The volume was also estimated by measuring linear dimensions of the rectangular bar for reference purpose. The measured density was converted to the relative density by comparing with the theoretical density of the pure copper ($8.96 \text{ g}\cdot\text{cm}^{-3}$) at room temperature.

Shrinkage is produced by the diffusion mechanisms including viscous flow, volume diffusion and plastic flow [29]. The shrinkage of sintered copper samples was evaluated as linear shrinkage and volumetric shrinkage by measuring the dimensions of the sample before and after sintering.

The microstructural features of the sintered samples were examined by microscopy. Magnified images were generated at lower magnification by reflected light microscopes (Olympus Transmitted/reflected Light Microscopes). Higher magnification images were generated via electrons by ESEM (FEI Quanta 600 FEG Environmental Scanning Electron Microscope) using an accelerating voltage of 20 kV. Weight percentage of Cu and O in the green and sintered copper samples was determined by EDX (Bruker Energy-dispersive X-ray spectroscopy).

To evaluate the strength of the final parts, tensile test specimens were printed with AcuPowder 500A copper powder and sintered in hydrogen/argon at various temperatures. The tensile test specimen was designed following "Standard Flat Unmachined Tension Test Specimens for Powder Metallurgy (P/M) Products" in ASTM E8 standard [30]. The printed dimension was scaled up by a scaling factor based on the average shrinkage detected in the similar sintering profile. The stress-displacement curve was obtained from an Instron (150 kN static rating) testing machine with a displacement rate of 50 mm/min.

3 Results and Discussion

3.1 Green part creation

Table 2 summarizes the powder information used in creating copper parts via Binder Jetting. The information on particle size distribution, weight percentage of copper element and the packing density was determined by the characterization techniques presented in Section 2.2. The particle size distribution and the powder morphology SEM pictures are shown in Figure 4 andFigure 5. The Ozometal atomized copper powder has the highest packing density because of the relatively wide particle size distribution.

Table 2. Powder particle size distribution, packing density and purity

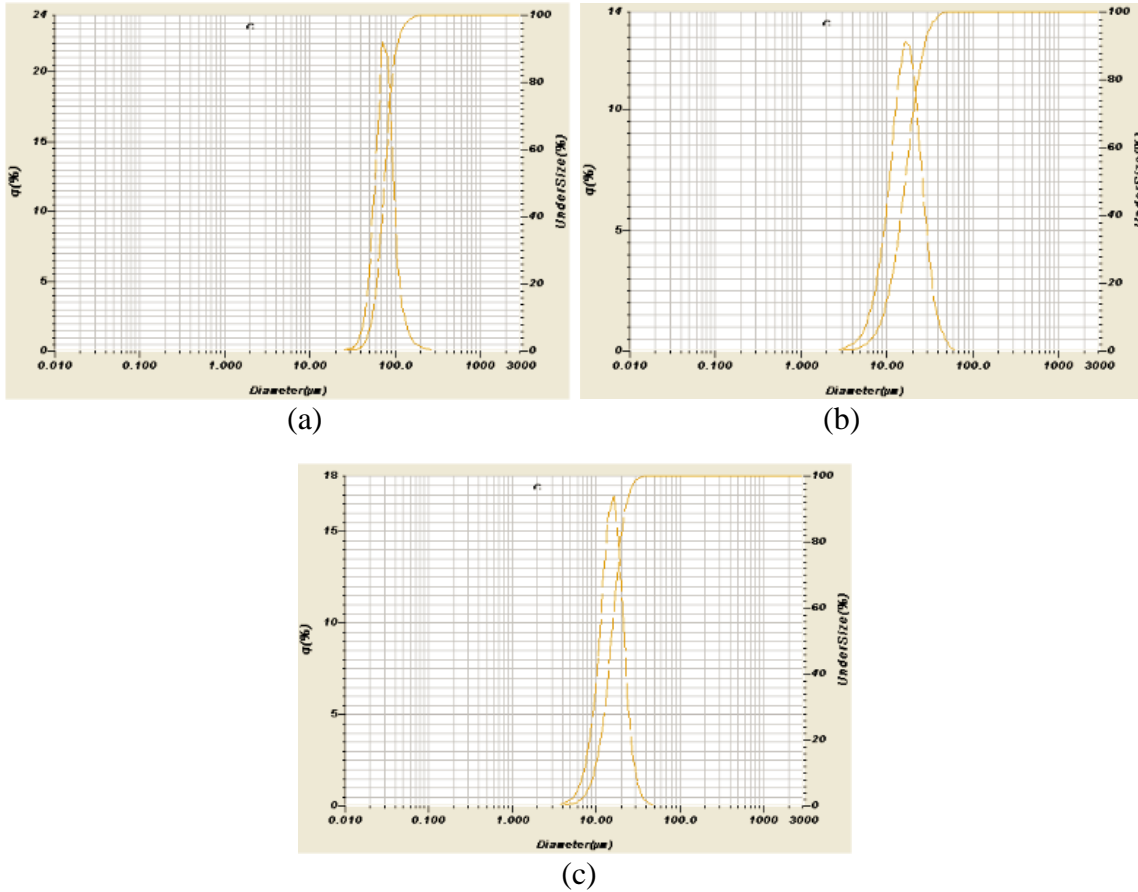| Powder name	Median particle size (μm)	Packing rate (% of theoretical density)	Purity (Cu wt. %)
AcuPowder 153A copper powder	75.2	55%	91.0%
Ozometal atomized copper powder	16.5	63%	95.3%
AcuPowder 500A ultra-fine atomized copper powder	15.3	56%	96.4%

(a)

(b)

(c)

Figure 4. Particle size distribution determined by laser scattering of (a) AcuPowder 153A copper powder (b) Ozometal atomized copper powder (c) AcuPowder 500A atomized copper powder
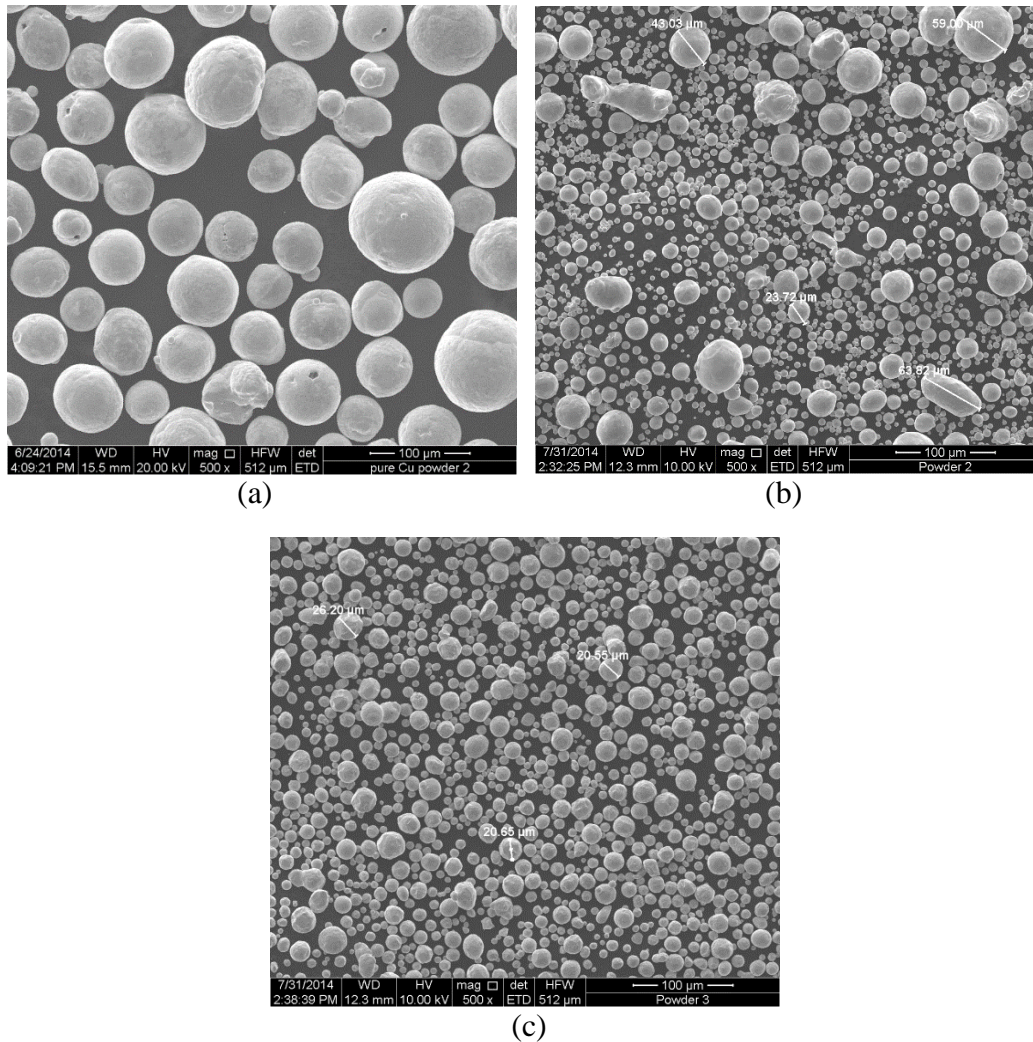
Figure 5. Powder SEM microscopy of (a) AcuPowder 153A copper powder (b) Ozometal atomized copper powder (c) AcuPowder 500A atomized copper powder

In a bench-top powder-binder interaction test where binder droplets were dispensed from a syringe onto a pile of powder, the binder was demonstrated to have a good wetting and penetrating characteristic with the atomized copper powders. Rectangular test specimens were successfully created by Binder Jetting on ExOne R2 3D printer with the settings listed in Table 3. The layer thickness and binder saturation were determined using the methods described in Section 2.3. The layer thickness was adjusted based on the median/largest particle size, and a binder saturation of 70% was demonstrated to have a good shape creation as well green part strength for all three powders. Two binder saturation ratios, 60% and 80%, were used for creating AcuPowder 500A copper powder to study the effect of binder saturation on sintering characteristics (Figure 10).

Table 3. Printing parameters in the green part creation

Powder name	Layer thickness (µm)	Binder saturation ratio (%)
AcuPowder 153A copper powder	100	70
Ozometal atomized copper powder	80	70
AcuPowder 500A ultra-fine atomized copper powder	80	60 and 80

3.2 Preliminary study on the sintering of copper printed via Binder Jetting

To identify the appropriate sintering profile for the printed copper green parts, the authors conducted a preliminary sintering study that leveraged post-processing procedures used in existing copper powder metallurgy research. In a sintering study of compacted copper powder, satisfactory densification was achieved in a temperature range from 750 °C to 1000 °C, and a maximum of 90% sintered density was observed when sintered at 1000 °C for 100 minutes [35]. In the sintering of copper powder in injection molding (MIM) fine oxide reduced copper with a median size of 10 µm was sintered below 1050 °C where a sintered density of 95% was achieved [32].

Figure 6. Sintered copper part samples (AcuPowder 153A copper powder sintered in pure hydrogen at 1000 °C for 8 hours)
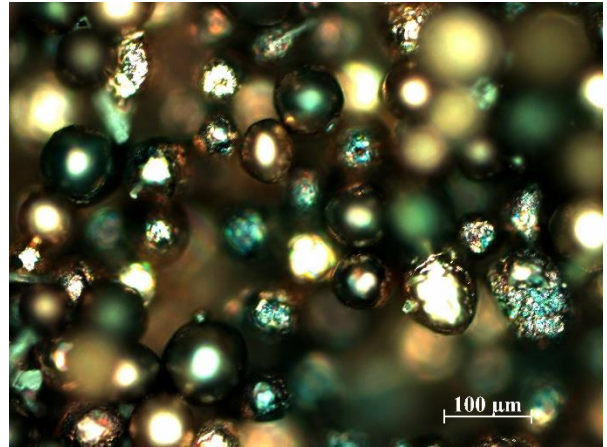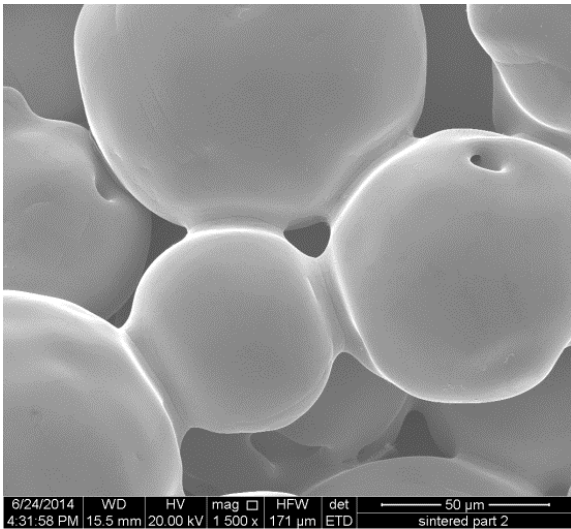
Figure 7. SEM (left) and optical microscopic (right) pictures showing the necks between particles formed in the initial sintering stage

When these same post-processing parameters were used on copper powder processed by Binder Jetting, the produced parts had significantly lower density. Figure 6 shows the samples made from AcuPowder 153A copper powder (74 median size) being fired at 1000 °C for 8 hours. The shrinkage after sintering was less than 5% and the sintered density was less than 60%. The SEM picture in Figure 7 shows the discrete particles and the sharply concave necks formed between particles. This is the evidence of an initial stage sintering where no significant densification effect and the recrystallization of the structure and pores was observed.

The difficulties in sintering copper prepared by Binder Jetting are not surprising given the large powder particle size and loose packing of the particles. These characteristics leave large spaces between particles which lowers the sinterability of solid state sintering. Similar results were found in prior work in using LS to process copper. In that work, the researchers looked to bimodal mixing of powders and polymer-coated powders to increase part density [2]. In this paper, the authors look to achieve higher part density by exploring different heating schedules and sintering atmospheres, and by using powders with various particle size distributions.

3.2 Densification and shrinkage

Due to the unsuccessful densification effort mentioned in the previous section, higher sintering temperatures were examined. Samples made from AcuPowder 153A copper powder and Ozometal atomized copper powder were sintered in air/vacuum air at temperatures ranging from 1060 °C to 1090 °C to explore its effect on volumetric shrinkage (Figure 8b) and part density (Figure 8a). Ozometal copper powder can be sintered to a significantly higher density than AcuPowder 500A due to the smaller size and wider distribution.
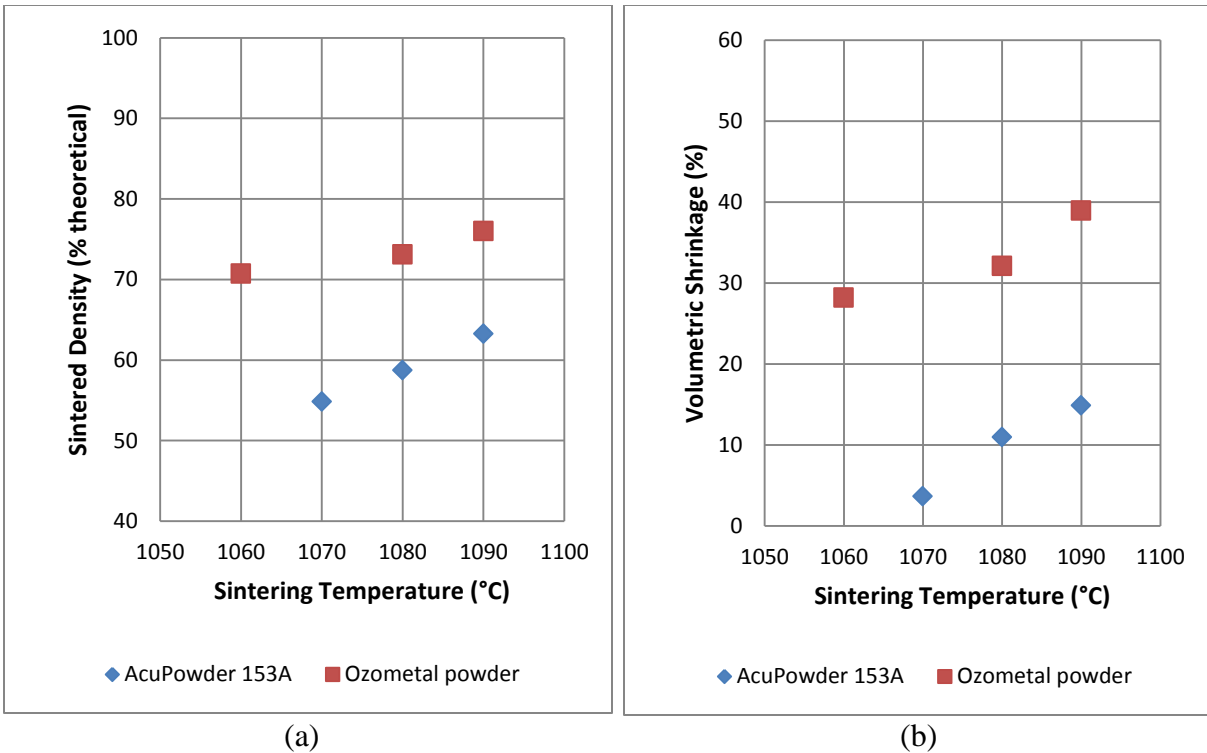
Figure 8. The relationship between densification and sintering temperature of AcuPowder 153A and Ozometal powder: (a) sintered density (b) volumetric shrinkage, sintered in air/vacuum for 4 hrs.

Finer copper powders, Ozometal copper powder and AcuPowder 500A, were sintered in hydrogen/argon atmosphere. The sintering temperature (Figure 9) and time (Figure 10) were varied to study their effects on the sintered density and shrinkage. In Figure 10, two different binder saturation ratios were sintered using same heating schedules.

Higher sintering temperature increased the final sintered density and shrinkage but was limited by the powder size and packing. Longer sintering time has the tendency to improve the densification. However in Figure 10 the best sintered density (85.5%) occurred at 4 hours instead of 6 hours. This observation needs further investigation by expanding to different powders and wider range of the sintering time. In Figure 10 the binder saturation did not have a major effect on densification; however more findings with respect to the binder saturation are discussed in Section 3.3. While it can be concluded that small particle size improves sinterability and sintered density, it is noted that the particle size distribution contributes to sinterability, as the wide size distribution in Ozometal atomized copper powder sintered to similar density of the finer powder.
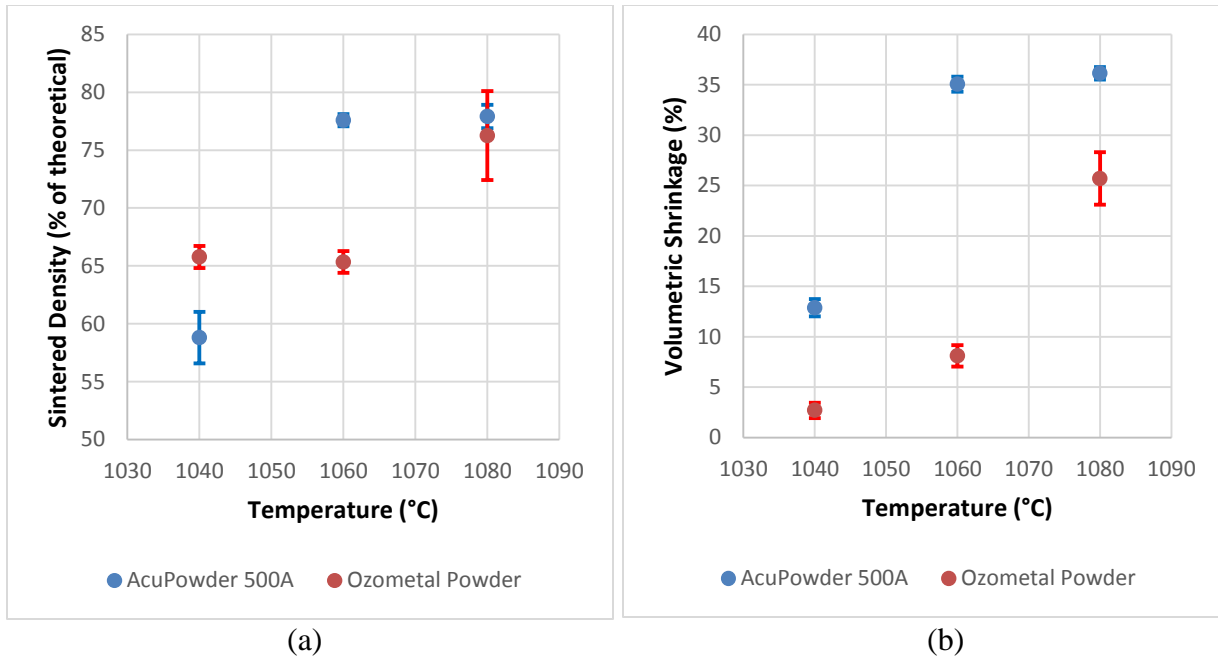
Figure 9. The relationship between densification and sintering temperature of AcuPowder 500A and Ozometal copper powder: (a) sintered density (b) volumetric shrinkage, sintered in hydrogen/argon for 2 hrs.
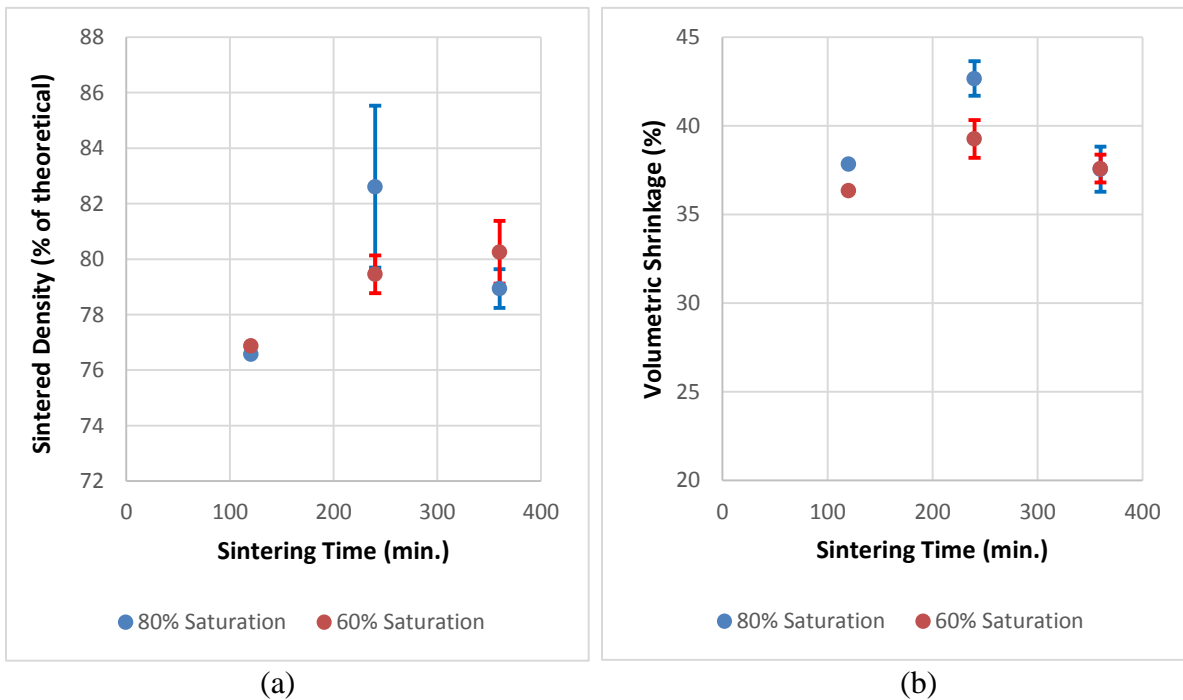

Figure 10. The relationship between densification and sintering time of AcuPowder 500A copper powder (60% and 80% saturation): (a) sintered density (b) volumetric shrinkage, sintered in hydrogen/argon at 1080 °C.

The highest achievable sintered density and volumetric shrinkage for the tested powders is shown in Table 4. It was noticed the copper samples being fired at high temperatures that are close to, or even higher than, the melting temperature of copper did not melt or lose the shape. This is caused by the powder impurity or copper oxidation layers, which can increase the powder melting temperature.

Table 4. The highest achievable sintered density and volumetric shrinkage

Powder name	Sintered profile	Sintered density (% theoretical)	Volumetric shrinkage (%)
AcuPowder 153A copper powder	1090 °C/240 min. Air/vacuum	63.2%	14.9%
Ozometal atomized copper powder	1080 °C/120 min. hydrogen/argon	77.6%	22.7%
AcuPowder 500A ultra-fine atomized copper powder	1080 °C/240 min. hydrogen/argon	85.5%	43.4%

For AcuPowder 153A copper powder, which is the coarsest powder among the three received powders (Table 1), the density after sintering increased from 55% to less than 65% and the volumetric shrinkage was less than 15%. The sintered density of a finer powder (Ozometal atomized copper powder) improved by 10% compared to the coarse powder, which reached an average of 74% of the pore-free copper density. The maximum sintered density of AcuPowder 500A ultra-fine atomized copper powder (the finest among three) was 85.5%.

3.3 Porosity type

Three different density measurement methods were used to determine sintered density. The volume calculated from the three dimensions of rectangular bars is a rough estimation for the bulk volume. The displacement volume measured by Archimedes' principal and gas pycnometry represents the bulk density only if the surface porosity is sealed by oil impregnation. For non-impregnated specimens, the bulk volume does not include the surface connected pores, which are filled with water or helium gas. In this paper the Archimedes' principle density of oil impregnated parts is used to measure the bulk density.

The authors noticed non-impregnated sintered parts have a nearly theoretical density of copper when measured by gas pycnometry. This result indicates that the majority of the pores in the sintered copper samples are surface-connected. This conclusion is also supported by examining the porosity of sintered copper under SEM (Figure 11).

In Binder Jetting, one droplet of binder jets into the powder bed and binds multiple particles together forming a primitive. In Figure 11 (a) and (b), one can tell the surface of the sintered part is composed of vertical lines (Y-direction) formed by stitching primitives together. In Figure 11 (c), the copper particles in the same primitive sintered to final stages where pores inside one primitive are very less. However, the diffusion and necking between adjacent primitives are very limited due to the large spacing between the primitives, leaving large pores in between. These

pores are inter-connected under microscope, and are also surface-connected due to the aforementioned findings. Based on these observations, future effort will be made to reduce spacing between primitives ("Y Spacing" in ExOne R2 software) to improve the sintered density of copper.
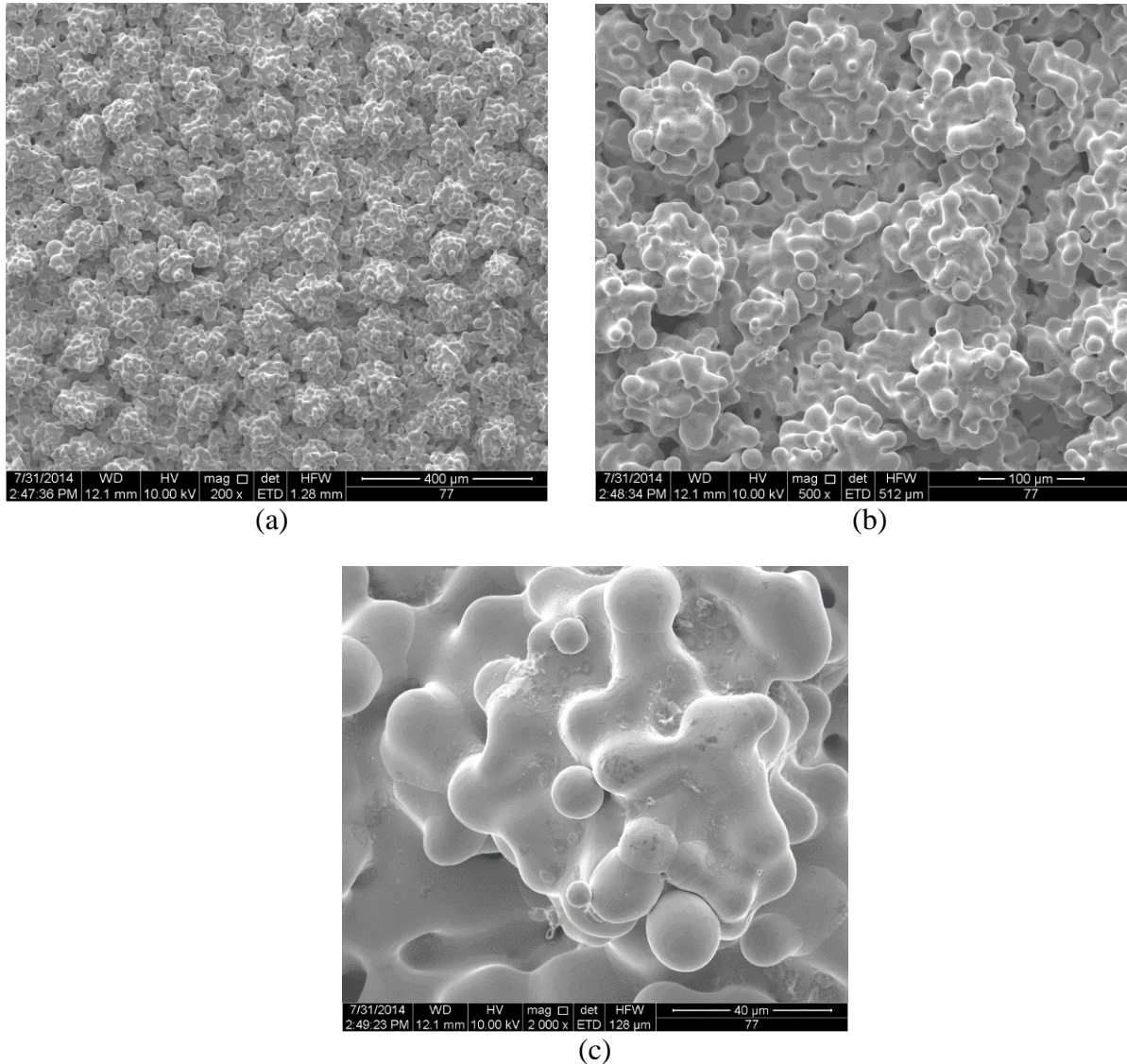

(a)

(b)

(c)

Figure 11. SEM of sintered AcuPowder 500A copper powder (1080 °C, 2 hours) at magnifications of (a) 200x, (b) 500x and (c) 2000x

3.4 Effects of reduction on sintering

A reducing atmosphere not only improves the purity of final products by reducing copper oxide, but also has a positive effect on sintering and densification. The relative degree of surface oxidation affects the final sintered density of copper powders [32,33]. The proper reduction process for sintering copper powders is to fully reduce the oxidation and remove the water vapor before the closure of pores during sintering [34,35]. It has been found that an isothermal holding

before reaching the relative density of 85%, or a holding temperatures no higher than 900 °C for most powders is appropriate [32].

To evaluate the effects of a reducing atmosphere, green parts made of AcuPowder 500A copper powder were sintered in controlled reducing atmosphere and non-reducing atmosphere (air with vacuum). The shrinkage and sintered density of these parts are compared in Table 5 . Compared to the non-controlled air atmosphere, the reducing atmosphere during sintering can improve the sintered density by more than 20% (Table 5). In the controlled reducing atmosphere, the densification was not significantly improved by increasing the concentration of hydrogen (Figure 12). While a reducing atmosphere can improve sintered density, the excessive supply of hydrogen than needed has not been demonstrated useful in improving densification.

Table 5. A densification comparison between sintering AcuPowder 500A copper powder in reducing and non-reducing atmospheres (1060 °C, 2 hours)

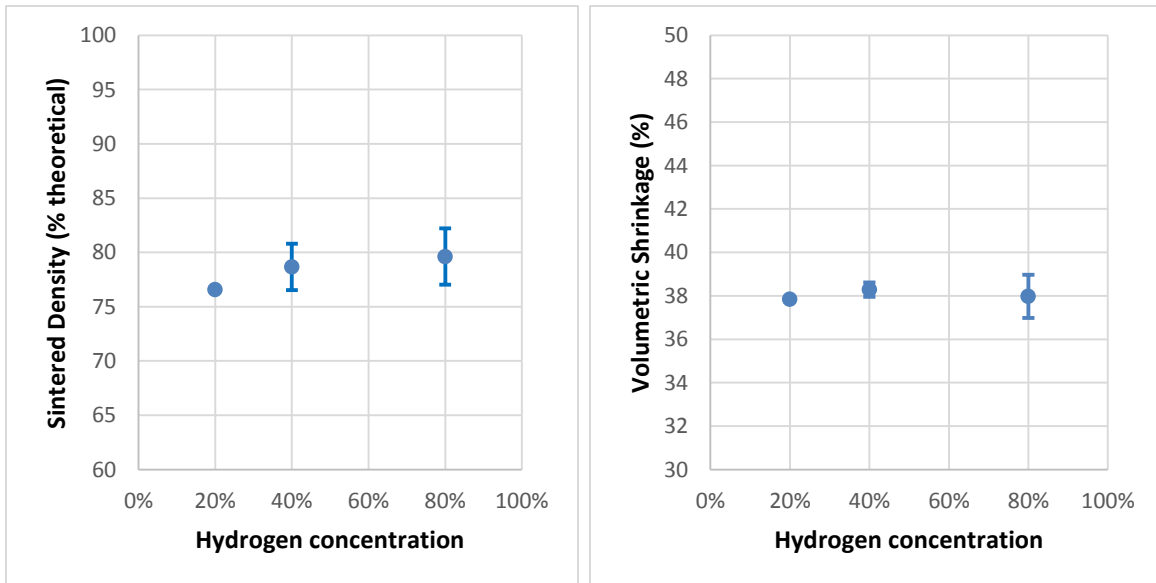|	**Volumetric shrinkage (%)**	**Sintered density (% theoretical)**
Sintering in non-reducing atmosphere (air with vacuum)	5.5	52.9
Sintering in reducing atmosphere (pure hydrogen)	37.1	78.2

Figure 12. Sintered density and shrinkage of AcuPowder 500A copper powder in controlled reducing atmosphere (1080 °C, 2 hours, 100 ml/cc flow rate)

3.4 Chemical composition

As described in Section 2.2, chemical composition analysis was conducted via EDX spectroscopy. The results of the analysis of printed green parts (AcuPowder 153A copper powder) without any heat treatment and parts that were sintered in hydrogen are presented in Table 6. As observed in these results, the reducing atmosphere increased the purity of the final

copper part, but was not able to completely convert copper oxide to its metal form during the sintering.

Table 6. Chemical composition comparison after sintering in a reducing atmosphere

	AcuPowder 153A (1000 °C for 4 hrs.)	Ozometal (1060 °C for 2 hrs.)	AcuPowder 500A (1080 °C for 2 hrs.)
Green parts	91.04% Cu	95.32% Cu	96.36% Cu
Sintered parts	94.94% Cu	97.32% Cu	97.11% Cu

3.5 Uniaxial tensile test

To evaluate the strength of the printed copper parts, a tensile test specimen was first designed following the ASTM E8 standard. The green part was printed larger to compensate for the shrinkage that would be caused by the sintering cycle (as determined in Section 3.2). The specimen was printed with AcuPowder 500A copper powder and was sintered at 1080 °C, 1060 °C and 1040 °C for 2 hours. As shown in Figure 12, the sintered specimen has a uniform shrinkage and the dimension of the sintered specimen was close to the ASTM standard.

Figure 12. Tensile test specimen: sintered at 1060 °C (top) sintered at 1080 °C (bottom)
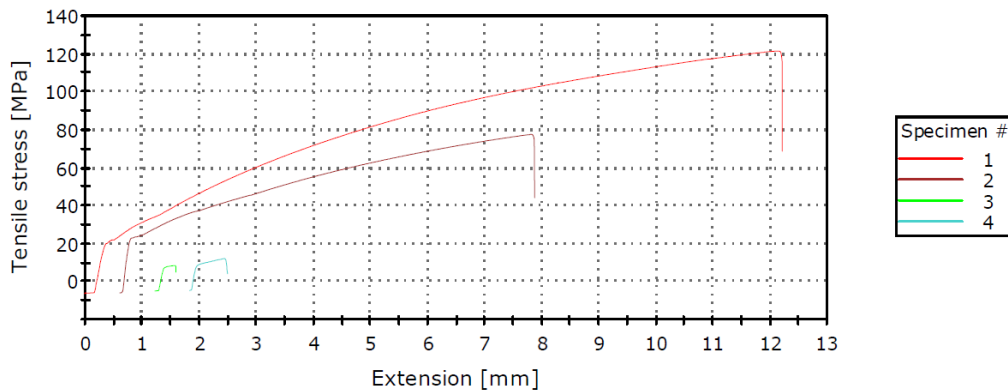

Figure 13. Engineering stress-extension curve of copper P/M parts made via Binder Jetting in the tensile testing

The ultimate tensile strength of different specimen is summarized in Table 9. Compared to the engineering data of copper (ultimate strength of 210MPa and a yield strength of 70MPa), the copper parts made by Binder Jetting have up to 55.6 % of the theoretical ultimate tensile strength of copper. The specimen displayed certain ductility, as demonstrated by the curve. One can tell the tensile properties of copper P/M made by Binder Jetting is proportional to its sintered density. A reduced density has a tremendous negative effect on the tensile strength.

Table 7. Tensile stress of specimen sintered with various temperatures

Specimen number	Sintering profile	Ultimate tensile strength (MPa)
1	1080 °C, 2 hours	116.7
2	1060 °C, 2 hours	73.3
3	1040 °C, 2 hours	8.4
4	1040 °C, 2 hours	6.9

The relatively low strength can be attributed to the parts' porosity, as previous studies have shown that the strength of porous sintered copper powder compacts is proportional to its porosity [2, 35]. To improve the mechanical strength of the copper fabricated via Binder Jetting, efforts need to be made in minimizing porosity or improving the densification during the sintering of copper.

4. Summary and future work

In this paper the Additive Manufacturing of copper via Binder Jetting was explored. Three purchased atomized copper powders were successfully printed on an ExOne R2 3D metal printer. The copper green parts were sintered in a tube furnace and a maximum of 85.5% of theoretical density has been achieved (Table 4). In the temperature range from 1060 °C to 1090°C the sintered density and shrinkage is proportional to the temperature (Figure 9). The reducing sintering atmosphere can achieve a purity of up to 97.3% (Table 6). The controlled sintering atmosphere with the presence of hydrogen can increase the purity of copper by up to 3.9% (Table 6) and can improve the sintered density by up to 25.3% (Table 5). The tensile strength of printed sintered copper parts was 55.6% of the theoretical value due to the porosity (Table 7).

In Binder Jetting, large particle size is preferred for powder spreading while fine powders are critical to the sinterability and have the potential advantages in improving resolution and surface quality. In was noticed one major challenge facing the Binder Jetting was to improve the sinterability and densification while the copper powders were relatively coarse and loosely packed. Therefore, future work will focus in the techniques that have the potential to improve copper sinterability while still maintaining good powder spreading. The authors will investigate multimodal mixture of powders, spray-dried granulated particles, and mixing sintering aids/inhibitors, etc. In addition, the authors will explore the effect of printing parameters on sintered part density and characteristics. Further characterization will be focused in the areas of microstructural features, structural integrity, and thermal/electrical conductivity.

5. Acknowledgement

6. References

[1]   Bourell, D. L., Beaman, J. J., Leu, M. C., and Rosen, D. W., 2009, "A Brief History of Additive Manufacturing and the 2009 Roadmap for Additive Manufacturing : Looking Back and Looking Ahead."

[2]   Badrinarayan, B., and Barlow, J. W., 1992, "Metal Parts From Selective Laser Sintering of Metal-Polymer Powders," Solid Freeform Fabrication Symposium, pp. 141–146.

[3]   Badrinarayan, B., and Barlow, J. W., 1991, "Selective Laser Sintering of a Copper-PMMA System," Solid Freeform Fabrication Symposium, pp. 245–250.

[4]   Murr, L. E., Gaytan, S. M., Ramirez, D. A., Martinez, E., Hernandez, J., Amato, K. N., Shindo, P. W., Medina, F. R., and Wicker, R. B., 2012, "Metal Fabrication by Additive Manufacturing Using Laser and Electron Beam Melting Technologies," J. Mater. Sci. Technol., **28**(1), pp. 1–14.

[5]   Ramirez, D. a., Murr, L. E., Martinez, E., Hernandez, D. H., Martinez, J. L., Machado, B. I., Medina, F., Frigola, P., and Wicker, R. B., 2011, "Novel precipitate–microstructural architecture developed in the fabrication of solid copper components by Additive Manufacturing using electron beam melting," Acta Mater., **59**(10), pp. 4088–4099.

[6]   Ramirez, D. a., Murr, L. E., Li, S. J., Tian, Y. X., Martinez, E., Martinez, J. L., Machado, B. I., Gaytan, S. M., Medina, F., and Wicker, R. B., 2011, "Open-cellular copper structures fabricated by Additive Manufacturing using electron beam melting," Mater. Sci. Eng. A, **528**(16-17), pp. 5379–5386.

[7]   Yang, L., Harrysson, O., West II, H., and Cormier, D., 2011, "Design and characterization of orthotropic re-entrant auxetic structures made via EBM using Ti6Al4V and pure copper," Solid Freeform Fabrication Symposium, pp. 464–474.

[8]   Mahale, T. R., 2009, "Electron Beam Melting of Advanced Materials and Structures (Doctoral dissertation)," North Carolina State University.

[9]   Sriraman, M. R., Gonser, M., Fujii, H. T., Babu, S. S., and Bloss, M., 2011, "Thermal transients during processing of materials by very high power ultrasonic additive manufacturing," J. Mater. Process. Technol., **211**(10), pp. 1650–1657.

[10]   Truog, A. G., Sriraman, R. M., and Babu, S. S., 2012, "Surface Modification of Very High Power Ultrasonic Additive Manufacturing (VHP UAM) Aluminum and Copper Structures," Trends in Welding Research, 9th International Conference, pp. 757–762.

[11]   Sriraman, M. R., Babu, S. S., and Short, M., 2010, "Bonding characteristics during very high power ultrasonic Additive Manufacturing of copper," Scr. Mater., **62**(8), pp. 560–563.

[12]   ASTM Standard F2792, 2013, "Standard Terminology for Additive Manufacturing Technologies."

[13]   Meisel, N. A., Williams, C. B., and Druschitz, A., 2012, "Lightweight Metal Cellular Structures via Indirect 3D Printing and Casting," Solid Freeform Fabrication Symposium, pp. 162–176.

[14]   Utela, B. R., Storti, D., Anderson, R. L., and Ganter, M., 2010, "Development Process for Custom Three-Dimensional Printing (3DP) Material Systems," J. Manuf. Sci. Eng., **132**(1), p. 011008.

[15]   Lam, C. X. F., Mo, X. M., Teoh, S. H., and Hutmacher, D. W., 2002, "Scaffold development using 3D printing with a starch-based polymer," Mater. Sci. Eng. C, **20**(1-2), pp. 49–56.

[16]   Leong, K. F., Cheah, C. M., and Chua, C. K., 2003, "Solid freeform fabrication of three-dimensional scaffolds for engineering replacement tissues and organs," Biomaterials, **24**(13), pp. 2363–2378.

[17]   Tay, B. Y., Zhang, S. X., Myint, M. H., Ng, F. L., Chandrasekaran, M., and Tan, L. K. A., 2007, "Processing of polycaprolactone porous structure for scaffold development," J. Mater. Process. Technol., **182**(1-3), pp. 117–121.

[18]   Suwanprateeb, J., and Chumnanklang, R., 2006, "Three-Dimensional Printing of Porous Polyethylene Structure Using Water-Based Binders," J. Biomed. Mater. Res. B. Appl. Biomater., **78**(1), pp. 138–145.

[19]   Lee, M., Dunn, J. C. Y., and Wu, B. M., 2005, "Scaffold fabrication by indirect three-dimensional printing.," Biomaterials, **26**(20), pp. 4281–9.

[20]   Cima, M. J., Yoo, J., Khanuja, S., Rynerson, M., Nammour, D., Giritlioglu, B., Grau, J., and Sachs, E. M., 1995, "Structural ceramic components by 3D printing," Solid Freeform Fabrication Symposium, Austin, TX, pp. 479–488.

[21]   Sachs, E. M., Hadjiloucas, C., Allen, S., and Yoo, H. J., 2003, "Metal and ceramic containing parts produced from powder using binder derived from salt," U.S. Patent 6,508,980 B1.

[22]   Snelling, D., Blount, H., Forman, C., Ramsburg, K., Wentzel, A., Williams, C., and Druschitz, A., 2013, "THE EFFECTS OF 3D PRINTED MOLDS ON METAL CASTINGS," Solid Freeform Fabrication Symposium, pp. 827–845.

[23]   Utela, B., Storti, D., Anderson, R., and Ganter, M., 2008, "A review of process development steps for new material systems in three dimensional printing (3DP)," J. Manuf. Process., **10**(2), pp. 96–104.

[24]   Sachs, E. M., 2000, "Powder dispensing apparatus using vibration.", U.S. Patent 6,036,777

[25]   Sachs, E. M., Cima, M. J., Caradonna, M. A., Grau, J., Serdy, J. G., Saxton, P. C., Uhland, S. A., and Moon, J., 2003, "Jetting layers of powder and the formation of fine powder beds thereby," U.S. Patent 6,596,224 B1.

[26]   Cima, M. J., Lauder, A., Khanuja, S., and Sachs, E., 1992, "Microstructural Elements of Components Derived From 3D Printing," Solid Freeform Fabrication Symposium, pp. 220–227.

[27]   ASTM Standard B923, "Standard Test Method for Metal Powder Skeletal Density by Helium or Nitrogen."

[28]   ASTM Standard B962, "Standard Test Methods for Density of Compacted or Sintered Powder Metallurgy (PM) Products Using Archimedes' Principle."

[29]   Alexander, B. H., and Balluffi, R. W., 1957, "THE MECHANISM OF SINTERING OF COPPER," ACTA Metall., **5**, pp. 666–677.

[30]   ASTM Standard E8, "Standard Test Methods for Tension Testing of Metallic Materials."

[32]   Chan, T.-Y., Chuang, M.-S., and Lin, S.-T., 2005, "Injection moulding of oxide reduced copper powders," Powder Metall., **48**(2), p. 129.

[33]   Ono, K., Kaneko, Y., and Kankawa, Y., 1994, "Effects of Oxidation on Debinding Process for Sintered Properties of Injection Molded Copper Powders," J. Japan Soc. Powder Powder Metall., **41**(3), pp. 227–231.

[34]   Lim, T., and Hayashi, K., 1991, "Effects of Addition of Al, Cr and Si on Complete Densification Characteristic in Sintering of Cu Fine Powder," J. Japan Soc. Powder Powder Metall., **38**(2), pp. 114–120.

[35]   Lim, T., and Hayashi, K., 1993, "Effects of Equilibrium Pressure of Gas Generated by Reduction Reaction in Sintering Densification of MIM Fine Powders," J. Japan Soc. Powder Powder Metall., **40**(4), pp. 373–378.

[36]   "ExOne," [Online]. Available: http://www.exone.com/en/materialization/systems.

[37]   "VoxelJet," [Online]. Available: http://www.voxeljet.de/en/systems/3d-druckervxc800/.